Transverse beam jitter damping along the Future Circular Collider e^+e^- injector linacs

S. Bettoni[*]
Paul Scherrer Institut, 5232 Villigen, Switzerland

A. Latina[†] and A. Grudiev
CERN, Meyrin, Switzerland

(Received 15 January 2025; accepted 28 May 2025; published 30 June 2025)

Transverse stabilization of the beam is crucial for optimizing the performance of a particle accelerator, regardless of its application. The most common method for minimizing transverse beam jitter is the Balakin-Novokhatsky-Smirnov (BNS) damping technique. Although this method has been successfully implemented worldwide, it has limitations since a significant fraction of the accelerating structures are operated off crest. In this work, we propose an alternative approach to induce the required energy spread, utilizing the natural curvature of the accelerating rf field in combination with a relatively long bunch and a longitudinal wakefield. This approach achieves strong damping of the transverse beam oscillations, similar to BNS damping, while simultaneously optimizing beam quality and maximizing acceleration efficiency. We have applied this method to the design of the Future Circular Collider injector linacs, designed to reach a beam energy of up to 20 GeV. However, this method is general and can be applied in principle to any accelerator.

DOI: 10.1103/8wx6-9spr

I. TRANSVERSE BEAM STABILITY

Orbit stabilization of particle beams in accelerators is critical for maintaining and optimizing the performance of accelerators, from high-energy physics colliders to light sources.

Shot-to-shot fluctuations in the transverse centroid—both in position and angle—can manifest either within a single bunch or between successive bunches. Several sources may contribute to the generation of these transverse oscillations. In the case of a linac downstream of a photoinjector, where the electron beam is initially generated, such variations may originate from laser beam jitter on the photocathode or from instabilities in the electron emission process itself. Analogous mechanisms are relevant for primary beams impinging on a target to produce positrons or other secondary particles, which are subsequently transported through downstream sections of the collider. In higher-energy regions, where the beam is extracted from the damping ring, transverse centroid oscillations in both position and angle may also arise due to fluctuations in the phase and amplitude of the extraction elements. The underlying physics mechanisms governing both multi-bunch and single-bunch scenarios are fundamentally the same. The key distinction lies in the source of the transverse deviations: in the multibunch case, this is driven by the off-axis or off-angle trajectory of preceding bunches, whereas in the single-bunch regime, it originates from intrabunch particle displacements in position and/or angle.

A beam deviating from the on-axis trajectory due to orbit jitter can lead to transverse emittance growth, as the beam exceeds the limits of the good-field region of magnets and due to feed-down effects. In this case, particles deviate from the optimal path within rf structures, leading to phase slippage relative to the rf field. This can result in inefficient acceleration, increased bunch energy spread, and potential particle loss, which can sometimes even result in machine activation and affect personnel safety. Furthermore, in complex accelerator systems that involve injection from one machine to another, such as from a linear accelerator (linac) to a circular booster, orbit jitter can drastically reduce an injection efficiency highly dependent on the beam pipe restrictions in regions designed to minimize disruption to the stored beam caused by the injection of new bunches and the capture of the particles in the unstable regions of the ring lattice. In colliders, a misalignment between the beams at the interaction point can significantly reduce the luminosity. In summary, maintaining control

[*]Contact author: simona.bettoni@psi.ch
[†]Contact author: andrea.latina@cern.ch

over the transverse beam jitter is essential to any accelerator. Therefore, the impact of the jitter must be included already in the accelerator's design phase, as a stable orbit ensures efficient operation, precision, safety, and optimal beam quality.

Beyond minimizing transverse jitter at the beam source, studying, predicting, and mitigating jitter amplification along the different accelerator sections is fundamental. This amplification is particularly pronounced in the case of high-charge bunches, where intensity-dependent effects such as wakefields, typically induced by structures like radio frequency (rf) cavities or changes in beam pipe aperture, impart transverse kicks to particles based on their position within or between bunches.

In Sec. II, we review the main aspects of the Balakin-Novokhatsky-Smirnov damping (BNS), the most widely used method to mitigate transverse beam jitter in electron linacs and storage rings [1–7]. This approach relies on generating an energy spread along the bunch, obtained by operating the rf cavities off crest. This solution presents some disadvantages for the final beam properties. In this work, we propose a different approach to induce the energy spread that achieves transverse jitter attenuation while mitigating the drawbacks of operating the rf cavities off crest.

In Sec. III, we define the concept of jitter amplification and give a brief overview of the Future Circular Collider electron-positron (FCC-ee) machine. In Sec. IV, we apply the proposed method to FCC-ee injector linacs. Finally, in Sec. V, we apply our approach to the design and optimization of the FCC-ee injector linacs. Using this method, we can maintain the jitter under control along all the linacs and fulfill all the requirements of the downstream sections.

II. THE BNS DAMPING

In a linear accelerator, particle beams undergo transverse betatron oscillations as they traverse the alternating focusing and defocusing fields of the quadrupole magnets. When a charged particle passes off axis through accelerator components such as rf cavities, it generates electromagnetic wakefields. These wakefields have a defocusing effect on the trailing particles, amplifying the beam's transverse oscillations, leading to beam degradation, orbit jitter amplification, or even beam breakup. These effects occur both between particles in the same bunch and between bunches. We refer to the first case as single-bunch effects induced by short-range wakefields and to the latter as a multibunch effect caused by long-range wakefields. Specific design measures can be implemented to mitigate these effects, such as optimizing the rf structure aperture, strengthening the beam optics, or, specifically for the long-range wakefield, incorporating a higher-order mode (HOM) suppression scheme. However, these measures only partially address the problem, as other counteracting factors, such as the overall footprint of the accelerator and the efficiency of power-to-beam energy conversion, also influence the choice of design parameters.

Historically, several accelerators have reported performance degradation due to orbit jitter. The Stanford Linear Collider (SLC), operated at the Stanford Linear Accelerator Center (SLAC) from 1989 to 1998, faced significant challenges in beam orbit stability, primarily due to its length and the high bunch charge required for collisions. SLC was a high-energy particle accelerator designed to collide electrons and positrons at a center-of-mass energy of approximately 91 GeV, or 45.5 GeV per beam, mainly to study the properties of the Z boson and electroweak interactions. At the time of its operation, this machine was the longest linear accelerator ever built, with a total length of 3.2 km. A major issue observed at the SLC was a strong beam jitter and beam degradation, bringing to beam breakup (BBU) instability [8].

A particularly effective method for mitigating BBU instabilities is the BNS damping. This technique works by introducing an energy spread along the beam, achieved by operating the rf structures off crest. By creating a controlled energy spread within the bunch, particles with different energies experience different focusing forces in the lattice of the machine, leading to a different phase advance of the particles. This phase advance difference causes destructive interference of the transverse oscillations, effectively damping the beam instabilities. BNS damping can be considered a form of Landau damping, but the main difference is that BNS damping relies on a correlated energy spread, whereas Landau damping exploits uncorrelated variations [9]. The SLC was the first large-scale application of BNS damping [10]. This technique successfully stabilized the electron and positron beams at SLC, becoming a key milestone in accelerators to be implemented in future linear collider projects [7].

However, BNS damping comes with several drawbacks. First, the typical off-crest phase required is between 15° and 20°. Consequently, the acceleration efficiency is reduced by approximately 4%–6% along the section where BNS is implemented and eventually where the induced energy chirp is removed. This may be significant in terms of cost, especially for long linacs. In addition, BNS damping, while beneficial in reducing transverse oscillations, increases the sensitivity to static misalignments of quadrupoles and rf structures, as also observed during the design of the FCC-ee linacs [11], being the transverse emittance growth larger for off-crest acceleration than for the on-crest case.

In this work, we propose an alternative to the off-crest rf operation used for BNS damping. We considered two distinct mechanisms to introduce energy spread into the beam: rf curvature and longitudinal wakefields. Depending on the beam parameters—such as bunch length and charge—and machine parameters—such as aperture of the rf structures and nominal focusing of the lattice—one mechanism may dominate over the other and both can be used to

obtain the desired energy spread. Also considering the strong dependence of the emittance growth on the operating phase of the rf structures, we did all the optimizations operating the rf structures on crest to minimize the impact of this deleterious effect. This aspect is advantageous also in terms of robustness of the stabilization to beam arrival time/phase jitter of the rf structures compared to the BNS damping approach. The bunch length was also optimized to introduce sufficient energy spread for effective damping of transverse beam jitter, while constraining the spread to a fraction of a percent in order to mitigate chromatic aberrations detrimental to beam quality. This optimization was carried out under specific machine constraints—most notably, the requirement to minimize beam manipulation, enabling sufficiently long bunches at the gun and booster injection stages, while achieving short bunches in the linac sections. Under these conditions, an optimal rms bunch length of approximately 1 mm was determined.

Our stabilization strategy uses the same principle of the BNS damping scheme, wherein the energy spread is introduced to induce a variation in betatron phase advance along the beam longitudinal coordinate to produce destructive interference of transverse oscillations, thereby suppressing jitter growth. However, unlike conventional BNS damping, which relies on off-crest rf operation, our method achieves the same stabilizing effect while maintaining on-crest operation with advantages on the acceleration efficiency and beam quality.

III. THE JITTER AMPLIFICATION FACTOR

When a bunch performs betatron oscillations, the transverse wakefields excited by the particles traveling off axis through the accelerator induce a deflecting kick to the trailing particles. In the case of an oscillation due to an incoming transverse jitter, these wakefield kicks can effectively increase the amplitude of the betatron oscillation, thereby amplifying the jitter.

The jitter amplification (JA) can be reduced, for example, by using strong focusing. However, strong focusing can be disadvantageous in terms of reduced filling factor, larger chromatic effects, tighter alignment tolerances, and, ultimately, the increased cost associated with counteracting these unwanted effects.

We identify it as a fundamental quantity associated with a beamline and the bunch charge since it results from the interplay between bunch charge, wakefield effects, and the lattice's focusing strength. Since it is a rather important quantity, we present a robust technique for evaluating and controlling it, using tracking simulations, which applies to any beamline. The approach involves transporting a set of test bunches through the beamline lattice, each initialized off axis in the canonical coordinates in the transverse horizontal plane $x - P_x$ (equivalently in vertical transverse plane $y - P_y$). The initial positions of the bunches are arranged to trace out a circle in the phase space, with the radius set to a fraction, typically, 10% of the initial beam size and divergence. Each bunch is then tracked independently through the beamline. At the beamline's exit, the area of the ellipse in the phase space formed by all the tracked bunches is calculated. The JA factor is determined as the square root of the ratio between the final and initial ellipse areas:

$$\mathrm{JA} = \sqrt{\frac{A_{\mathrm{final}}}{A_{\mathrm{initial}}}}. \tag{1}$$

Assuming, for example, an initial rms jitter in position δx_0 and in angle δ_0', and the jitter amplification JA along a section, the jitter downstream that section will be at most:

$$\begin{aligned} \delta x_1 &= \delta x_0 \cdot \mathrm{JA}, \\ \delta x_1' &= \delta x_0' \cdot \mathrm{JA}. \end{aligned} \tag{2}$$

For a perfectly linear lattice without wakefield effects, the JA factor remains constant at the value of 1. In the presence of wakefield effects, the JA factor tends to increase.

As an example of this phenomenon, we tracked a 5 nC bunch through a test linac obtained from the FCC-ee high-energy linac (see following sections for details), lowering the phase advance of its FODO cells from 90° to 60°. We tested the cases with and without short-range wakefields. Figure 1 shows that, when wakefield effects are considered, the area of the ellipse increased from 56 to 168 mm eV/c, that is, by a factor ≈3, resulting in a jitter amplification factor JA ≈ $\sqrt{3}$. Figure 1 presented an example of JA

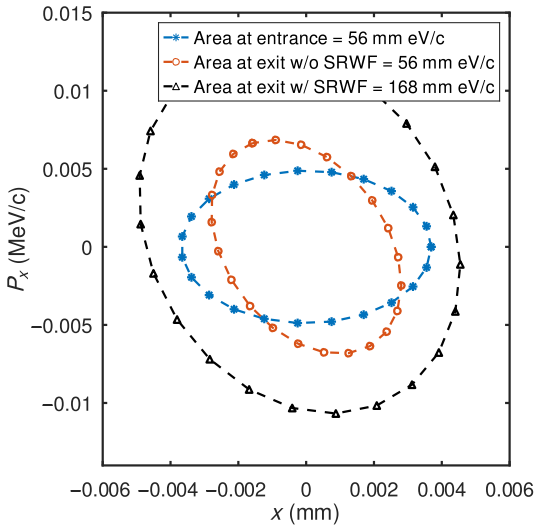

FIG. 1. Evaluation of the jitter amplification in a test linac. The asterisks indicate the phase space coordinates of each test bunch at the linac start; the triangles and the circles show the corresponding coordinates at the linac end, with and without short-range wakefields (SRWF), respectively. As reported in the legend, when SRWF effects are considered, the ellipse area increases by a factor ≈3, giving a JA ≈ $\sqrt{3}$.

caused by short-range wakefields. However, JA is also induced by multibunch phenomena, such as long-range wakefields. In the case of long-range effects, the JA factor must be computed bunch-by-bunch using multibunch beam tracking.

The JA factor possesses three significant properties worth highlighting. First, it accounts for jitter amplification in both the position and angular axes, independently of the phase advance between the input and output of the lattice. Second, its evaluation does not require the knowledge of the Twiss parameters, which may be difficult to estimate, e.g., in the presence of strong rf focusing. Third, for oscillations well within the beamline aperture, the JA factor is independent of the amplitude of the incoming transverse jitter. These properties make the JA factor a robust and powerful metric of a beamline's stability, particularly useful when the absolute incoming beam jitter is unknown, which is typically the case in the initial design phase of an accelerator.

The jitter amplification factor of a machine, JA, is the product of the jitter amplification factors $(\mathrm{JA})_k$ of each section:

$$\mathrm{JA} = \prod_{k=1}^{N} (\mathrm{JA})_k. \tag{3}$$

Using this formulation, the contribution of each section to the overall beam behavior can be evaluated independently. Once the absolute amplitude of the initial transverse beam jitter is known, the expected beam jitter can be determined at any point along the accelerator. Conversely, given a specific jitter requirement at the end of a beamline, the JA factor enables the calculation of the allowable beam jitter tolerance at the beamline start. Equation (3) is valid for the single-bunch, $\mathrm{JA}_{\mathrm{Single}}$, and multibunch, $\mathrm{JA}_{\mathrm{Multi}}$, effects, and the total jitter amplification is given by the product of these quantities:

$$\begin{aligned}\mathrm{JA}_{\mathrm{TOT}} &= \mathrm{JA}_{\mathrm{Single}} \cdot \mathrm{JA}_{\mathrm{Multi}} \\ &= \left[\prod_{k=1}^{N} (\mathrm{JA})_k\right]_{\mathrm{Single}} \cdot \left[\prod_{k=1}^{N} (\mathrm{JA})_k\right]_{\mathrm{Multi}}.\end{aligned} \tag{4}$$

All the simulations presented in this work were performed using RF-Track [12], a tracking code developed at CERN. RF-Track enables the simulation of linacs, accounting for both single- and multi-bunch effects in single- and multi-bunch beams. Additionally, it allows for the evaluation of JA at any longitudinal position z along the accelerator, as well as the tracking of sliced bunch properties, such as emittance, energy spread, Twiss parameters, etc.

The method described so far applies solely to uncoupled motion. In the presence of $X-Y$ coupling, e.g., due to solenoids in the lattice, JA must be extended considering the variation of the volume of the four-dimensional phase space $X-P_x-Y-P_y$ rather than the variation of the area of a two-dimensional ellipse. The approach outlined in this section will be employed to describe the proposed stabilization method for the linacs discussed in the remainder of this paper.

IV. THE FUTURE CIRCULAR COLLIDER ELECTRON-POSITRON

The Future Circular Collider is a proposed next-generation electron-positron collider, part of an ambitious plan to extend the frontiers of particle physics beyond the capabilities of the Large Hadron Collider (LHC) and its future upgrades.

A top view of the expected future CERN accelerator concept is shown in Fig. 2. The FCC-ee will be installed in a circular tunnel approximately 91 km in circumference, located in the Geneva region near CERN, across the Swiss-French border. The collider is planned to operate at various energy stages, each tailored to study specific particles. The electron-positron collisions are significantly cleaner compared to the hadronic ones, allowing for more precise measurements of particle interactions and properties. The energy of the collisions will be variable, depending on the performed study. The key parameters of the FCC-ee's main ring at each energy stage are shown in Table I. FCC-ee is envisioned as the initial phase of the larger Future Circular Collider (FCC) project, with a subsequent phase involving the construction of a proton-proton collider called Future Circular Collider hadron-hadron (FCC-hh). The FCC-hh aims to achieve an unprecedented beam energy of around 100 TeV, pushing the boundaries of high-energy physics. If the project will be approved, the construction of FCC-ee could begin in the late 2030s, with operational activities possibly starting in the 2040s. The proton-proton collider is expected to start operations in the 2070s and continue through the following decades.

The schematic layout of the FCC-ee injector complex sections relevant to the discussion in this work is presented in Fig. 3. A photoinjector [13], based on a Cs_2Te

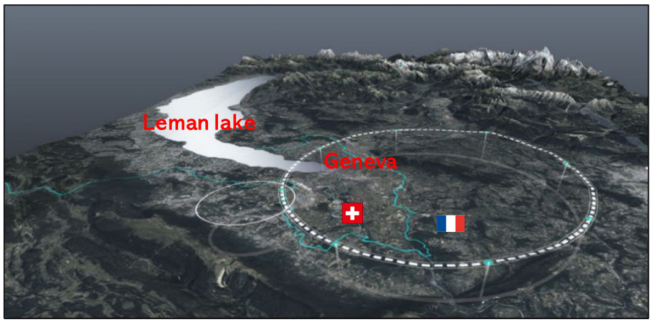

FIG. 2. Expected top view of the FCC-ee accelerator complex. The machines will span between France and the Geneva surroundings in Switzerland. The light blue line corresponds to the Switzerland-France border. The smallest ring shows the LHC.

TABLE I. Most significant parameters of the FCC-ee main ring. The data were reported during the FCC week held in the summer of 2024.

	Z	WW	ZH	$t\bar{t}$	Unit
Beam energy	45	80	120	182.5	GeV
Number of bunches/ring	10000	880	248	36	
Luminosity per IP ($\times 10^{34}$)	182	19.4	7.3	1.3	$cm^{-2}\,s^{-1}$
Luminosity/year for 4 IPs	8	18	6	10	$ab^{-1}/year$

photocathode, generates four bunches separated by 25 ns with a maximum charge of 5 nC each before entering the electron linac. This linac increases the electron beam energy from 200 MeV to 2.86 GeV. At this stage, the electron bunches can either be directed toward a target for positron production and acceleration (in the positron linac up to 2.86 GeV) or injected into a 2.86 GeV damping ring (DR). The DR is crucial for the massive reduction of the large emittance of the positron beam generated from the target, having a beneficial emittance reduction also for the electron beam, allowing generating a flat beam required by the downstream rings for both species and improving the beam orbit stability. Upon extraction from the DR, both the positron and electron beams are further accelerated up to 20 GeV in the high-energy (HE) linac before being transported along a several-kilometer-long transfer line to the booster ring, where the beam energy is ramped up according to the selected study following Table I.

V. THE JITTER AMPLIFICATION ALONG THE FCC-EE LINACS

The beam exiting both the electron linac and the HE linac must meet the specifications set by the downstream sections. The maximum allowable jitter at the exit of the electron linac is constrained by the acceptable loss in positron yield, defined as the number of positrons produced normalized to the number of electrons colliding on the target in cases where the electron beam is utilized for positron production. If the electron beam is instead sent to the HE linac and subsequently to the booster ring, the maximum acceptable jitter is determined by the transfer line at its exit and the ring injection efficiency. Table II summarizes the target design/tolerated beam parameters and the machine settings for both scenarios. According to Eq. (2), the jitter at each section can be computed from the JA obtained by tracking simulations, knowing the initial jitter. Presently, we assume as initial orbit jitter the value measured at the exit of the AWAKE gun section at about 200 MeV [14], where beam parameters are comparable to those of the start of the FCC-ee electron linac. In AWAKE, at this location, an orbit jitter of $0.12 \cdot \sigma$ was reported [15].

Since a complete damping ring (DR) design at the recently updated energy is underway, specifications for the acceptable jitter are not available yet. However, we expect the tolerance not to be so stringent, as the DR acceptance must be very large to capture the orders of magnitude larger positron transverse beam sizes. Furthermore, we expect that the damping will strongly reduce jitter. This allows us to neglect the jitter contributions upstream of the DR in the computation of the total final jitter for FCC-ee when the bunches are sent toward the booster ring.

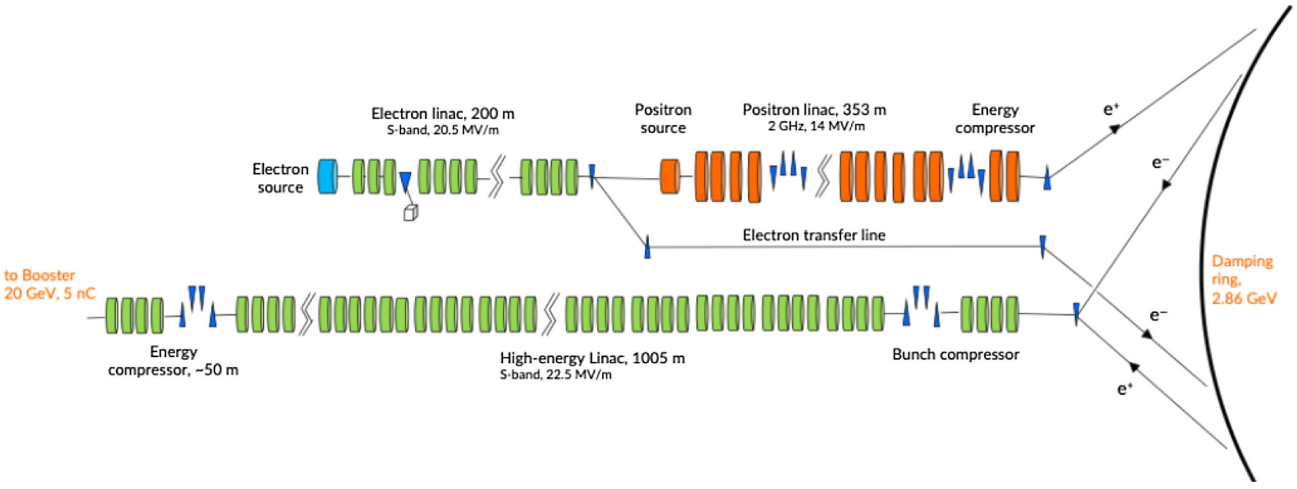

FIG. 3. Schematic layout of the FCC-ee injector complex. On the right side, the damping ring (DR) is visible, whereas on the left, the electron and positron beam generation system (upper part) and the higher-energy section for both the species (lower part) to the booster ring are indicated.

TABLE II. Beam and linacs design and target parameters. We state the jitter in terms of the beam transverse size σ. The beam longitudinal parameters are matched to those required by the booster using an energy compressor downstream of the HE linac like the one successfully in operation at SuperKEK-B [16] in combination with a low-level rf system. The rf structures properties has been optimized for cost, reliability of the machine, and beam quality [17,18].

	e^- linac	HE linac
Initial energy (GeV)	0.2	2.86
Final energy (GeV)	2.86	20
Species	e^-	e^- and e^+
Target energy spread (%)	< 2–3	0.1–0.15
Target rms bunch length (mm)		4
Design rms bunch length (mm)	1	1
Maximum jitter at the exit ($1/\sigma$)	0.17 [19]	1 [20]
FODO phase advance/cell (degrees)	90	90
Distance among quadrupoles (m)	3.75	3.75
rf frequency (GHz)	2.8	2.8
rf structure gradient (MV/m)	20.5	22.5
rf average aperture (mm)	16.1	12.9
rf structure length (m)	3	3
rf operating phase	On crest	On crest

Using Eqs. (3) and (4), we can compute the contribution of the different sections to the total jitter amplification. In the case where the electron beam is utilized for positron production, the total JA is equivalent to that of the electron linac, denoted as JA_e. In contrast, when the electron beam is directed to the booster ring, additional terms coming from the DR and the HE linac must be considered. We expect that the DR does not contribute to the increase, but it even reduces JA, because of the radiation damping, and that the injection and extraction kickers add a negligible jitter in angle considering the kicker systems available in the facilities currently running. From these considerations, we conclude that the major contributions to the JA are given by the linacs.

In accelerators, short- and long-range transverse wakefields may amplify an initial jitter presently unavoidable at the particle generation. The underlying physics driving the jitter amplification is the same for the two cases. In the design phase, however, these effects are typically addressed differently. After determining the JA for both the single- and the multi-bunch case, we compute the total one as the product of the two according to Eq. (4). We, therefore, determine the acceptable rf and lattice parameters, given the total JA budget along the linacs and at the interfaces with the downstream sections. In the following section, we describe the procedure and present our results.

A. Single-bunch dynamics

The transverse short-range wakefield is responsible for the effects of the particles within the same bunch. The Bane [21] formula is a widely recognized expression that describes the transverse wakefields caused by short-range point-charge wakefield, $W_T(s)$, in disk-loaded accelerating structures:

$$W_T(s) = \frac{4Z_0 c s_{00}}{\pi a^4}\left[1 - \left(1 + \sqrt{\frac{s}{s_{00}}}\right) \times \exp\left(-\sqrt{\frac{s}{s_{00}}}\right)\right], \tag{5}$$

where s is the longitudinal coordinate along the bunch, Z_0 the free space impedance, c the speed of light in vacuum, a the rf structures aperture radius, and s_{00} is obtained by a fitting procedure, and it is given by

$$s_{00} = 0.169\frac{a^{1.79} g^{0.38}}{p^{1.17}}, \tag{6}$$

where g is the gap between two subsequent irises, and p is the period of the rf structures. Fixed the frequency of the rf structures, a is the main parameter influencing the wakefield. The optics of the lattice, particularly the betatron phase advance per cell in the case of a FODO and the length of the single cell (distance among the quadrupoles), influence the impact of the wakefield on the beam. We determined the JA along the linacs varying the ratio of a over the rf wavelength of the accelerating structure, λ, and we verified the impact of the distance among the quadrupoles by tracking studies performed following the approach described in Sec. III.

Figure 4 shows the evolution of the jitter amplification along the electron linac for several of the apertures considered for studies performed on emittance growth due to static effects. These studies determined $a/\lambda = 0.15$ as the optimal rf aperture. This case corresponds to a final JA equal to almost 1.4 and a final jitter of about $0.17\,\sigma$, assuming the initial jitter of AWAKE. An important

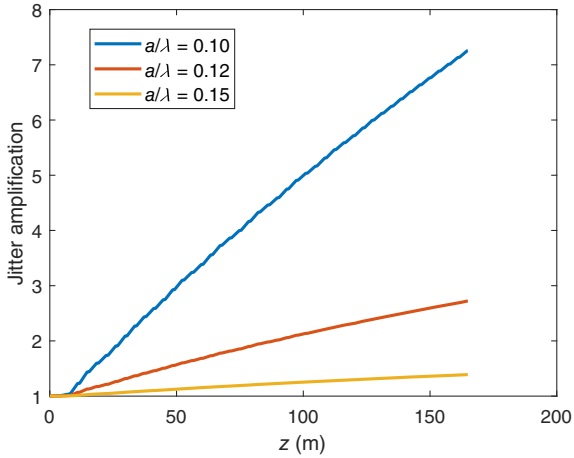

FIG. 4. Jitter amplification along the electron linac. The rf structures are operated on crest. The distance among the quadrupoles is 3.75 m.

TABLE III. FCC-ee electron linac final jitter amplification as a function of a, assuming different distances among the quadrupoles.

a/λ	a (mm)	JA	JA
		$d_Q = 3.75$ m	$d_Q = 4.75$ m
0.10	10.71	7.13	11.66
0.12	12.86	2.66	3.70
0.15	16.07	1.38	1.58

TABLE IV. FCC-ee HE linac final jitter amplification as a function of a, assuming different distances among the quadrupoles.

a/λ	a (mm)	JA	JA
		$d_Q = 3.75$ m	$d_Q = 4.75$ m
0.10	10.71	1.21	1.88
0.11	11.76	1.06	1.52
0.12	12.86	0.98	1.31

parameter in the design is the distance between the quadrupoles, d_Q. If this distance is increased, assuming a longer structure (this being beneficial for the effective shunt impedance), the final jitter would increase too. In Table III, several rf geometries assuming different d_Q are compared. Figure 5 shows the evolution of JA along the HE linac for several rf apertures. The derivative of JA in the case of the electron linac is positive along the full length of the section, indicating that the effect of the transverse wakefield on the jitter is dominant over any damping effect. The opposite scenario is observed in the case of the HE linac, where JA reaches a maximum before diminishing along the HE linac, indicating the presence of two counteracting phenomena: the amplification of the jitter and a damping effect. The previous design determined $a/\lambda = 0.12$ as the optimal rf aperture based on the transverse emittance growth due to static effects. This case would correspond to a JA equal to about 1, therefore producing a final jitter very close to the initial one. This, assuming a relatively small jitter coming from upstream sections (extraction kicker and DR), should reasonably provide a transverse jitter at the exit of the HE linac much below the maximum tolerated one. If the distance between the quadrupoles is increased to 4.75 m, the final jitter would be more than 30% larger, as it may be concluded from the data reported in Table IV. The transverse damping is expected in the case that BNS damping is performed operating the rf structures off crest; however, we achieved it operating the structures on crest, thereby obtaining all the advantages without the disadvantages previously described.

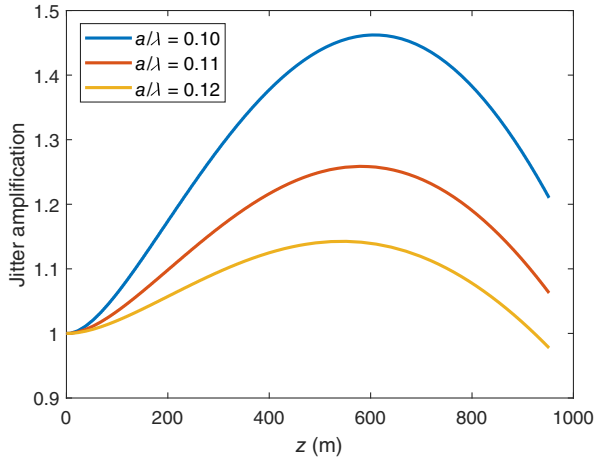

FIG. 5. Jitter amplification along the HE linac. The rf structures are operated on crest. The distance among the quadrupoles is 3.75 m.

Before discussing the approach proposed in this work and its sensitivity to the most critical machine and beam parameters in detail, we show the results for the multibunch dynamics. These effects must be included in the calculation of the total beam transverse jitter.

B. Multibunch dynamics

To perform multibunch simulations, we artificially imposed a varying kick from a trailing bunch to the subsequent ones to simulate the long-range wakefield. Once the tolerated jitter is known, we quantify the maximum kick associated with the long-range wakefield. The maximum kick determined from our simulations is used for the optimization of the rf design. A significant advantage of this approach is that it allows for the evaluation of wakefield interactions that occur irrespective of the time separation between successive bunches. The approach may be applied even in the relatively initial phase of the design before knowing precisely this number, which may necessitate careful and long optimizations.

Figure 6 shows JA as a function of the kick imparted by the first bunch on the subsequent both for the electron and the HE linac. The only parameters that can be adjusted to reduce the JA are the HOM suppression during the rf structure design phase and the beam optics during the lattice optimization. The first effectively impacts solely the multibunch case, whereas the latter influences both single- and multi-bunch studies. HOM suppression mitigates the detrimental effects of the higher-order electromagnetic modes excited in resonant cavities by passing high-charge particle beams. However, this approach comes with certain drawbacks. The optimization process must ensure that the fundamental mode is not degraded, and it adds complexity to the design. The impact of the distance among the quadrupoles is a simpler way to mitigate the JA if foreseen during the design phase, as shown in Fig. 7, even if more space must be allocated to be able to include them in the lattice. The most favorable solution involves the use of shorter rf structures; however, this approach is associated

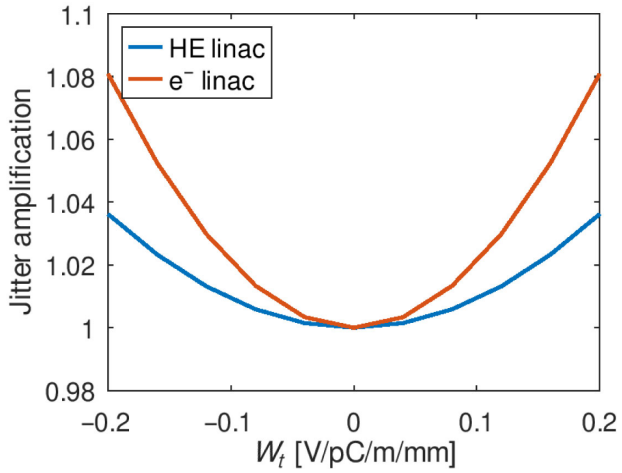

FIG. 6. Multibunch jitter amplification for the electron and the HE linac.

with a reduced shunt impedance [17] and a more expensive lattice, as more rf structures and quadrupoles are required to achieve the same final beam energy. Alternatively, maintaining relatively long rf structures and installing quadrupoles around them may become cost prohibitive due to the typically larger aperture required in such configurations. We obtained an acceptable compromise using rf structures of 3 m length and optics providing 90° FODO phase advance per cell. During the previous phase of the FCC-ee design, the rf structures were optimized to ensure a maximum kick of 0.11 V/pC/m/mm [17]. In the current design (different length of the linacs, DR also for the electrons, and at higher energy), this optimization translates

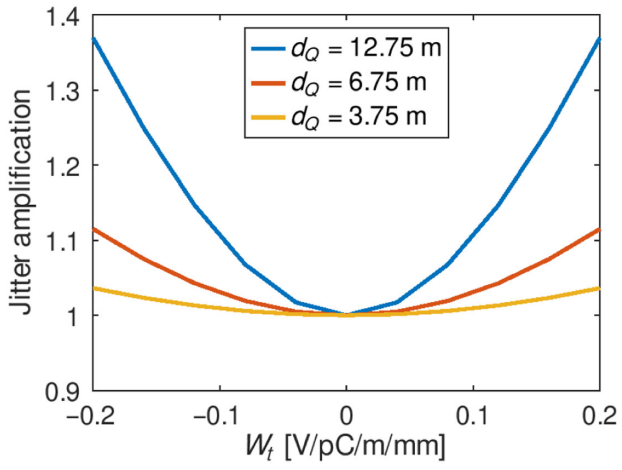

FIG. 7. HE linac multibunch jitter amplification as a function of the length of the structure, corresponding to a different distance among the quadrupoles. The length of the rf structures are 3, 6, and 12 m, respectively. Previous machines, like SLC, were designed with a distance among the quadrupoles of slightly more than 12 m. This implies a much larger JA than that of the FCC-ee HE linac (length of the structures equal to 3 m) at the same bunch charge and rf aperture.

to JA values of 1.38 and about 1 for the electron linac and the HE linac, respectively.

C. The damping mechanism

The booster ring downstream of the HE linac requires a relatively long bunch length on the order of 4 mm to mitigate instabilities due to the interaction of the beams with the accelerator. In the previous FCC-ee design iterations, no bunch compression system was incorporated between the gun section exit at 200 MeV and the end of the HE linac at 20 GeV. Therefore, a relatively long bunch was also beneficial to lower transverse emittance at the gun section exit. While a longer bunch length is beneficial in the upstream and downstream sections of the HE linac, this may be harmful in the linacs due to chromatic effects induced by the energy spread along the bunch impinged by the rf curvature of the accelerating structures and the longitudinal wakefield. A shorter bunch length may be beneficial because it reduces the impact of the transverse wakefield on the jitter but, at the same time, increases the energy spread along the bunch due to the longitudinal wakefield. Figure 8 shows the comparison of the relative energy spread of bunches with varying bunch lengths along the HE linac for the maximum design bunch charge of 5 nC. The single-bunch longitudinal wakefield induces a head-tail energy loss determined by the convolution of the bunch's current profile with the point-charge longitudinal wakefield. This effect is more pronounced for shorter bunch lengths. According to our simulations, a bunch length of about 1 mm provides a good balance among the various competing effects, as shown in Fig. 9.

As previously described, BNS damping, relying on a correlated energy spread impinged along the bunch, is a highly effective method for mitigating transverse beam jitter. However, BNS damping brings some disadvantages,

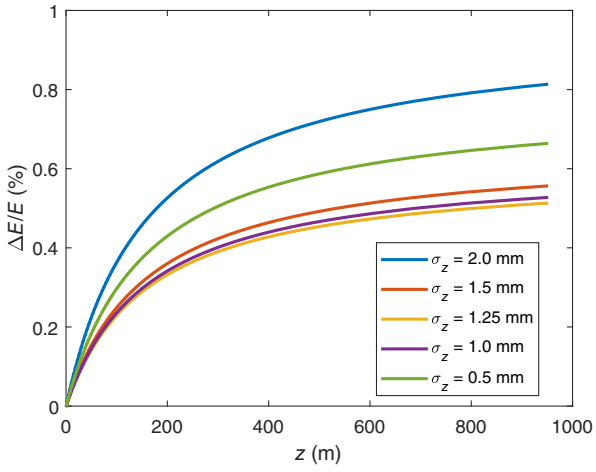

FIG. 8. Relative energy spread for different bunch lengths along the HE linac, assuming the maximum bunch charge. The rf structures are operated on crest.

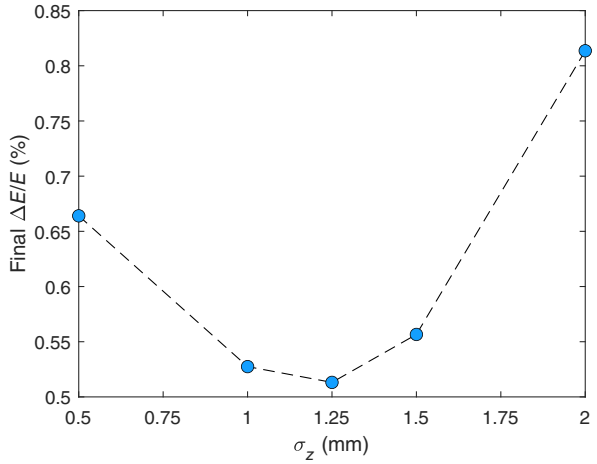

FIG. 9. Relative energy spread as a function of the bunch length at the HE linac exit, assuming the maximum bunch charge. The rf structures are operated on crest.

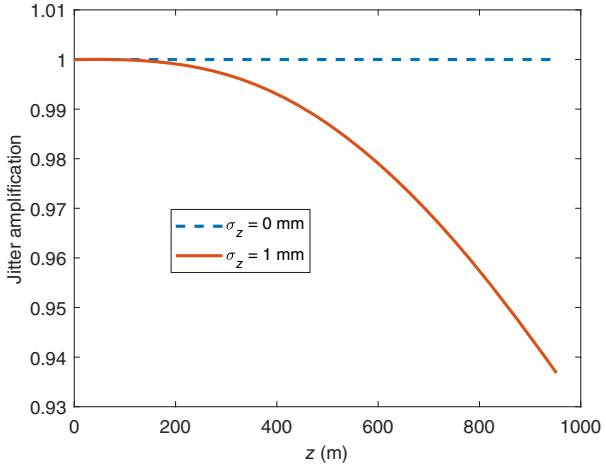

FIG. 10. Comparison of the JA evolution along the HE linac excluding the short-range wakefields in the calculations for the nominal and the *null* bunch length configuration.

which we discussed before due to the off-crest operation of the rf structures. We propose employing a relatively long bunch compared to the phase variation associated with the rf wavelength of the structures to exploit the energy spread generated by the rf curvature while operating the cavities on crest. This approach retains the benefits of BNS damping while avoiding its associated drawbacks. In the following discussion, we focus on the single-bunch case, but the same conclusions are valid for the multibunch scenario.

Two opposing phenomena affect the beam as it travels through the linacs: the transverse wakefield, which amplifies any initial transverse beam jitter, and the damping mechanism, which reduces it. To isolate the effect of the latter, we artificially removed the transverse wakefield in the simulations, and we computed the JA along the HE linac for the nominal bunch length of 1 mm and an ideal *null* bunch length case. The latter is not physical, assuming that all the particles composing the bunch start to move simultaneously, but it is a useful configuration for the following considerations. Figure 10 shows that in the case of the longer bunch, the JA is reduced compared to the *null* bunch length configuration. This is due to the energy spread increase induced by the finite bunch length and rf curvature, assuming our parameters (1 mm bunch length with rf structures operating at 2.8 GHz). This configuration gives results on the beam similar to the BNS damping. However, in this case, the energy spread is solely determined by the rf curvature, as the short-range wakefield was excluded from the simulations.

We now consider a more realistic scenario where short-range wakefields are also taken into account. As illustrated in Fig. 11, two distinct regimes are identified. In the first one, spanning from $z = 0$ m to approximately 500 m, the transverse wakefields contribute to an increase of JA. In contrast, the second one, extending from around 500 m to the end of the HE linac, exhibits a different behavior: not only does the JA cease to increase, but it is further reduced. As illustrated in Fig. 11, the significant reduction in JA is predominantly attributed to the influence of longitudinal wakefields, while the contribution of rf curvature is comparatively less.

The BNS damping approach is typically described with a two-particle model. Our method may be schematized using a three-particle system. Let's assume that the bunch is split into three sub-bunches along its longitudinal coordinate: the head (H), the center (C), and the tail (T). We also assume that each particle has 1/3 of the total charge for simplicity without losing generality. The energy spread along the bunch after that the bunch travels through the rf cavities can be expressed as

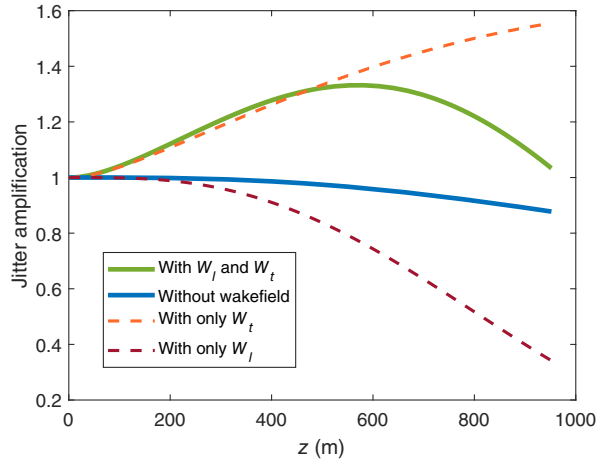

FIG. 11. Illustration of the two scenarios: short-range wakefield effects on JA as a function of position along the linac assuming the design parameters. The case without the short-range wakefields and with solely the transverse or the longitudinal component are also reported.

$$\begin{cases} \Delta E_H = -\Delta \mathrm{rf}_H + \Delta W_H \\ \Delta E_C = 0 \\ \Delta E_T = -\Delta \mathrm{rf}_T - \Delta W_T \end{cases}, \tag{7}$$

where the terms of the kind of $\Delta \mathrm{rf}_j$ correspond to the variation of energy induced by the rf curvature, and those of the kind of ΔW_k represent the ones associated with the longitudinal wakefield. The sign indicates that the energy variation is reducing (or increasing) the energy compared to that at the center, which is taken arbitrarily as a reference. To summarize, in our design, we use the rf curvature (which depends on the bunch length) and the short-range wakefield (which depends on the bunch charge and the bunch length) to damp the effect of the short-range transverse wakefield on JA. As for BNS damping, the cumulative energy variation along the bunch induces changes in the optical functions of the beam as it propagates through the linac. Figure 12 shows the horizontal beta-beat for the bunch head and tail while the beam travels along the HE linac. From $z \approx 400$ m, the beta-beat increases progressively until $z = 600$ m. Beyond this point, its envelope remains nearly constant. Within this range, the damping mechanism dominates over the transverse jitter amplification. Subsequently, transverse jitter amplification becomes the primary effect, persisting until the end of the high-energy (HE) linac. A similar trend is observed from the plot in Fig. 11.

The associated beta-beat is of the order of a few percent, small enough to be tolerated by the downstream transfer line but enough to damp the transverse jitter coming from the preceding section. Figure 13 shows the corresponding phase advance difference computed with respect to that of the center of the bunch along the HE linac. The asymmetry

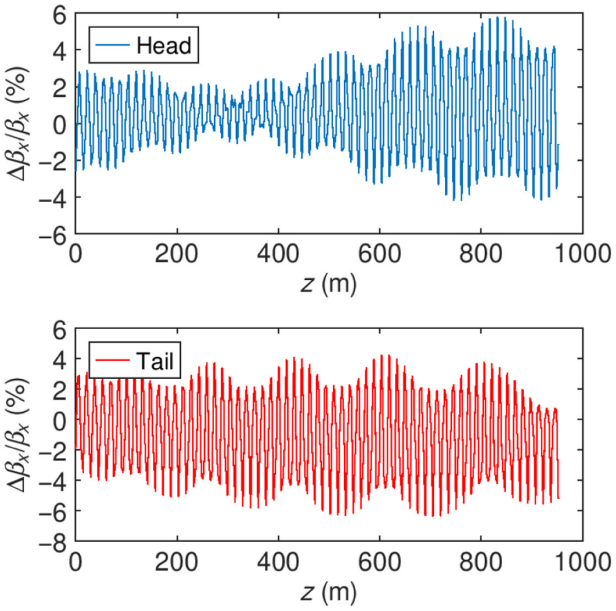

FIG. 12. Beta-beat of the beam (head and tail) assuming the center of the bunch as the reference along the HE linac.

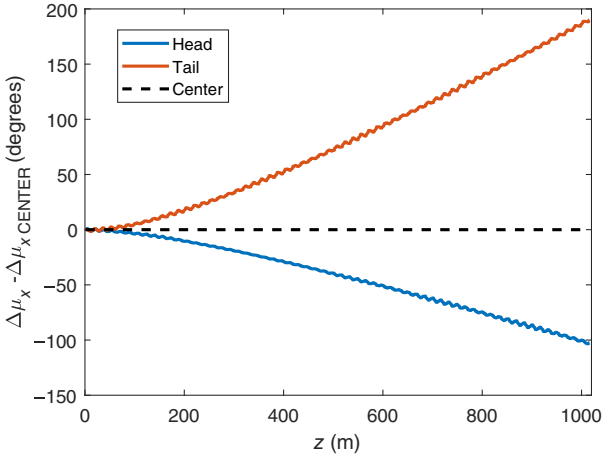

FIG. 13. Horizontal phase advances of head and tail with respect to bunch center along the HE linac.

and the different sign of the phase advance at the head and the tail with respect to the center of the bunch are other indications that the longitudinal wakefield dominates the induced energy spread. The difference of the phase advance with respect to the center of the bunch is more pronounced for particles at the tail than at the head. This results in a larger phase advance difference at the tail than at the head, as visible in Fig. 13. The effect of the rf curvature would have indeed given a symmetric distribution of the energy spread along the bunch instead.

The proposed method results in an energy variation along the bunch associated with a relatively moderate maximum rms energy spread of about 0.5% (important for other effects, like the emittance growth due to static misalignment, for example). The final value of the energy spread and bunch length are matched to the target booster parameters using a dedicated device at the end of the HE linac. Another advantage of employing a relatively large bunch length is the reduction in longitudinal decompression of the beam required to fulfill the booster specifications. This minimizes the effects associated with strong bunch compression, providing an optimal beam for injection to the transfer line first and to the booster after.

VI. CONCLUSIONS

The control of the transverse beam jitter is a fundamental aspect of any accelerator design for any application. A widely recognized method to minimize this effect is the BNS damping, which introduces a controlled energy spread. This approach has been used both in the past and in the present to damp transverse jitter efficiently. However, it is associated with several drawbacks due to the off-crest operation of the rf accelerating structures, the degraded quality of the transverse beam, and the acceleration efficiency. We propose using an alternative strategy to induce the necessary energy spread. Our method is expected to utilize a similar mechanism of BNS damping, thereby providing

transverse jitter damping but using on-crest operation of the rf structures, eliminating many of the drawbacks associated to the BNS damping scheme. We applied this approach to the design of the FCC-ee injector linacs, where we achieved a final transverse jitter comparable to the initial one for the injection to the downstream sections. This method is particularly effective for longer linacs, where the issue of transverse jitter amplification is more critical, and the energy spread along the bunch can accumulate over a sufficient distance. With appropriate adjustments to the lattice parameters and, when applicable (e.g., in machines operating with relatively long bunches), to the bunch length, this strategy may, in principle, represent a viable approach for stabilizing a wide range of accelerators.

ACKNOWLEDGMENTS

The authors would like to express their gratitude to the members of the FCC-ee Working Package 1, in particular to P. Craievich, A. Kurtulus, S. Doebert, R. Zennaro, and J.-Y. Raguin, for their contributions to the discussions throughout this study, and to the Swiss Accelerator Research and Technology (CHART) for financing the FCC-ee injector design study effort. This work was supported by funding from the European Union's Horizon 2020 research and innovation program under the European Union's Horizon 2020 research and innovation program grant agreement No. 951754.

DATA AVAILABILITY

The data that support the findings of this article are not publicly available. The data are available from the authors upon reasonable request.

[1] V. E. Balakin, A. V. Novokhatsky, and V. P. Smirnov, Vlepp: Transverse beam dynamics, in *Proceedings of the 12th International Conference on High-Energy Accelerators, HEACC 1983 : Fermilab, Batavia* (Fermilab, 1983), pp. 119–120, https://inspirehep.net/files/7fed12b8dcaaf3525cc37cf50b56a545.

[2] G. Guignard and J. Hagel, Multibunch BNS damping and wakefield attenuation in high frequency linacs, CERN Technical Report No. CERN SL 96-60 (AP) and CLIC Note 312, Geneva, 1996, https://cds.cern.ch/record/311231/files/sl-96-060.pdf.

[3] R. D. Ruth, Beam dynamics in linear colliders, Part. Accel. **30**, 33 (1990), https://cds.cern.ch/record/201938/files/p33.pdf.

[4] M. Aicheler *et al.*, *A Multi-TeV Linear Collider Based on CLIC Technology: CLIC Conceptual Design Report* (CERN, CERN Yellow Reports: Monographs, Geneva, 2012).

[5] M. Aicheler *et al.*, *The Compact Linear Collider (CLIC)—Project Implementation Plan* (CERN, CERN Yellow Reports: Monographs, Geneva, 2018), p. 247.

[6] C. Adolphsen *et al.*, The International Linear Collider Technical Design Report - Volume 3.II: Accelerator Baseline Design, 2013, https://inspirehep.net/literature/1240418.

[7] J. Seeman, D. Schulte, J. P. Delahaye, M. Ross, S. Stapnes, A. Grudiev, A. Yamamoto, A. Latina, A. Seryi, R. T. García, S. Guiducci, Y. Papaphilippou, S. A. Bogacz, and G. A. Krafft, in *Design and Principles of Linear Accelerators and Colliders* (Springer International Publishing, Cham, 2020), pp. 295–336.

[8] O. H. Altenmueller, E. V. Farinholt, Z. D. Farkas, W. B. Herrmannsfeldt, H. A. Hogg, R. F. Koontz, C. J. Kruse, G. A. Loew, and R. H. Miller, Beam break-up experiments at SLAC, in *Proceedings of the Linear Accelerator Conference, Los Alamos, New Mexico, USA* (1966), p. 267, https://accelconf.web.cern.ch/l66/papers/vi-02.pdf#search=%20domain%3Daccelconf%2Eweb%2Ecern%2Ech%20%20%2Bauthor%3A%22Altenmueller%22%20%20url%3Aaccelconf%2Fl66%20FileExtension%3Dpdf%20%2Durl%3Aabstract%20%2Durl%3Aaccelconf%2Fjacow.

[9] A. Novokhatski, BNS damping, in *Proceedings of the ICFA mini-Workshop, Zermatt, Switzerland* (2019), pp. 68–73, https://cds.cern.ch/record/2751715/files/10.23732_CYRCP-2020-009.68.pdf.

[10] J. T. Seeman, F.-J. Decker, R. L. Holtzapple, and W. L. Spence, Measured optimum BNS damping configuration of the SLC linac, in *Proceedings of the 1993 IEEE Particle Accelerator Conference, Washington, DC* (1993), p. 3234, https://accelconf.web.cern.ch/p93/PDF/PAC1993_3234.PDF.

[11] S. Bettoni *et al.*, FCC week 2023, https://indico.cern.ch/event/1202105/contributions/5383357/attachments/2661311/4610449/2023_FCCWeek_Bettoni_Def.pdf, 2023.

[12] A. Latina, RF-track reference manual (2024), 10.5281/zenodo.4580369.

[13] Z. Vostrel and S. Doebert, Design of an electron source for the FCC-ee with top-up injection capability, Nucl. Instrum. Methods Phys. Res., Sect. A **1063**, 169261 (2024).

[14] E. Gschwendtner *et al.*, The AWAKE Run 2 programme and beyond, Symmetry **14**, 1680 (2022).

[15] S. Doebert (private communication).

[16] SuperKEK-B Technical Design Report, https://www-linac.kek.jp/linac-com/report/skb-tdr/.

[17] A. Kurtulus, A. Grudiev, A. Latina, S. Bettoni, P. Craievich, and J.-Y. Raguin, Accelerating structures for the FCC-ee pre-injector complex: RF design, optimization, and performance analysis, in *Proceedings of the 32nd Linear Accelerator Conference (LINAC2024), Chicago, IL, USA* (2024), p. MPPB036, https://cds.cern.ch/record/2921864/files/document.pdf.

[18] H. W. Pommerenke, A. Grudiev, A. Latina, S. Bettoni, P. Craievich, J.-Y. Raguin, and M. Schaer, RF design of traveling-wave accelerating structures for the FCC-ee pre-injector complex, in *Proceedings of the 31st International Linear Accelerator Conference (LINAC2022), Liverpool, UK* (2022), https://accelconf.web.cern.ch/linac2022/papers/thpojo08.pdf.

[19] F. Alharthi and I. Chaikovska (private communication).

[20] Y. Dutheil (private communication).

[21] K. Bane, Short-range dipole wakefields in accelerating structures for the NLC, SLAC Technical Report No. SLAC-PUB9663 LCC-0116, 2003.